

# Study of the Structural and Magnetic Characteristics of Epitaxial Fe<sub>3</sub>Si/Si(111) Films

I. A. Yakovlev<sup>a,\*</sup>, S. N. Varnakov<sup>a,b</sup>, B. A. Belyaev<sup>a-c</sup>, S. M. Zharkov<sup>a,c</sup>,  
M. S. Molochev<sup>a</sup>, I. A. Tarasov<sup>a,b</sup>, and S. G. Ovchinnikov<sup>a-c</sup>

<sup>a</sup> Kirensky Institute of Physics, Siberian Branch, Russian Academy of Sciences, Krasnoyarsk, 660036 Russia

\* e-mail: yia@iph.krasn.ru

<sup>b</sup> Reshetnev Siberian State Aerospace University, Krasnoyarsk, 660014 Russia

<sup>c</sup> Siberian Federal University, Krasnoyarsk, 660041 Russia

Received March 28, 2014

The results of the structural and magnetic studies of the epitaxial structure prepared during the simultaneous evaporation from two iron and silicon sources on an atomically pure Si(111)7 × 7 surface at a substrate temperature of 150°C have been presented. The epitaxial structure has been identified as a single-crystal Fe<sub>3</sub>Si silicide film with the orientation Si[111]||Fe<sub>3</sub>Si[111] using methods of the X-ray structural analysis, transmission electron microscopy, and reflection high-energy electron diffraction. It has been established that the epitaxial Fe<sub>3</sub>Si film at room temperature has magnetic uniaxial anisotropy ( $H_a = 26$  Oe) and a relatively narrow uniform ferromagnetic resonance line ( $\Delta H = 11.57$  Oe) measured at a pump frequency of 2.274 GHz.

DOI: 10.1134/S0021364014090124

**1.** Thin films of the Fe–Si system attract rather high interest of researchers owing to their unique physical properties and prospects of their application in spintronics devices [1–4]. In magnetic metals such as iron or permalloy, the degree of electron spin polarization is about 40–45%. It was already demonstrated that the high degree of spin polarization of electrons in silicon can be created by their injection from a ferromagnetic metal electrode. The lower threshold of the spin polarization is 30% [5]. However, the possibility of the spin transfer decreases sharply due to the uncontrolled formation of different silicides on the interface of such structures [6, 7].

This problem can be solved by creating high-quality ferromagnetic Fe<sub>3</sub>Si silicide. According to calculations, it is a ferromagnetic semimetal with the spin polarization at a level of 43% and rather high Curie temperature of 577°C [8]. The formation of the completely epitaxial structure on the basis of silicon is of the highest interest. On one hand, this is due to the closeness of the interplanar distances (111) of silicon and iron silicide for the epitaxial growth ( $d_{\text{Si}} = 0.3138$  nm (PDF 4+ card #00-005-0565),  $d_{\text{Fe}_3\text{Si}} = 0.3271$  nm (PDF 4+ card #04-015-3939), Si(111)||Fe<sub>3</sub>Si[111] [9]). On the other hand, a larger electron mean free path is expected in the single-crystal tunnel layers than in the polycrystalline structures.

The main aim of this work was determining the technological conditions for the formation of ferromagnetic Fe<sub>3</sub>Si silicide and finding the ferromagnetic resonance parameters.

**2.** The Fe<sub>3</sub>Si structure was prepared by the method of thermal evaporation in superhigh vacuum on the boron-doped atomically pure substrate Si(111) (the resistivity of 5–10 Ω cm) on an Angara modernized molecular-beam epitaxy device [10]. The base vacuum in the technological chamber was  $1.3 \times 10^{-8}$  Pa. The substrate was subjected to chemical treatment before synthesis with subsequent thermal annealing in superhigh vacuum. The chemical treatment based on the technique proposed in [11] included three stages: the process of degreasing, the removal of the natural oxide from the Si substrate, and the formation of the passivating film of SiO<sub>2</sub> oxide with a thickness of ~1.5 nm on the Si surface. After the chemical treatment, the substrate was placed in superhigh vacuum, where it was subjected to the thermal annealing.

In the process of thermal annealing, the Si(111) plate was heated gradually for 3 h to 650°C at a rate of 4°C per minute and exposed at this temperature for 15 min. The pressure in the chamber did not increase higher than  $5.6 \times 10^{-7}$  Pa. Then, the substrate was heated sharply to 800°C with the exposure of 30 s. After that, the temperature was lowered again to 650°C. These “pulses” were performed until the additional reflections from the reconstructed surface Si(111)7 × 7 appeared in the reflection high-energy electron diffraction pattern, which indicated the preparation of the atomically pure silicon surface. Then, the substrate temperature was lowered to 150°C and was preserved for 60 min prior to evaporation.

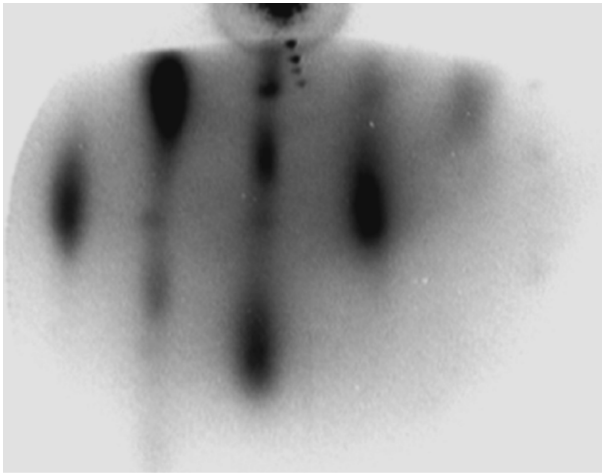


**Fig. 1.** Reflection high-energy electron diffraction pattern from the surface after the deposition of the  $\text{Fe}_3\text{Si}/\text{Si}(111)$  structure.

The simultaneous evaporation of iron and silicon was performed by the method of thermal evaporation from two Knudsen effusion cells made of high-temperature boron nitride. The deposition rates of separate materials were calibrated by the method of laser ellipsometry. The rate ratio  $\text{Si} : \text{Fe} \approx 0.57$  stoichiometric for  $\text{Fe}_3\text{Si}$  was provided. The process of the formation of the structure was controlled in situ on a LEF-751M laser ellipsometer [12] and by reflection high-energy electron diffraction.

The reflection high-energy electron diffraction pattern from the surface after the deposition of the structure shown in Fig. 1 demonstrates reflections in the form of dots, which are elongated in the vertical direction. This indicates the presence of the structure on the surface, which consists of single-crystal epitaxially formed islands with their heights smaller than the size of the base. The interplanar distances  $d = 0.192 \pm 0.010$  and  $0.143 \pm 0.010$  nm were obtained from the preliminary identification of the reflection high-energy electron diffraction pattern. They are close to the interplanar distances for the bulk phase of  $\text{Fe}_3\text{Si}$  [9],  $d_{(220)} = 0.20028$  nm and  $d_{(400)} = 0.14162$  nm.

**3.** The ex situ determination of the structural perfection and phase composition of the samples was performed using the methods of transmission electron microscopy on a JEM-2100 microscope (JEOL) [13] and X-ray structural analysis on a D8 ADVANCE powder diffractometer ( $\text{Cu}K_\alpha$ -radiation, Ni filter) with a VANTEC linear detector. The magnetic properties were studied on a scanning spectrometer of ferromagnetic resonance [14] at a pump frequency of 2.274 GHz.

Figure 2 shows the cross-sectional transmission electron microscopy image of  $\text{Fe}_3\text{Si}/\text{Si}(111)$  obtained on the high-resolution transmission electron micro-

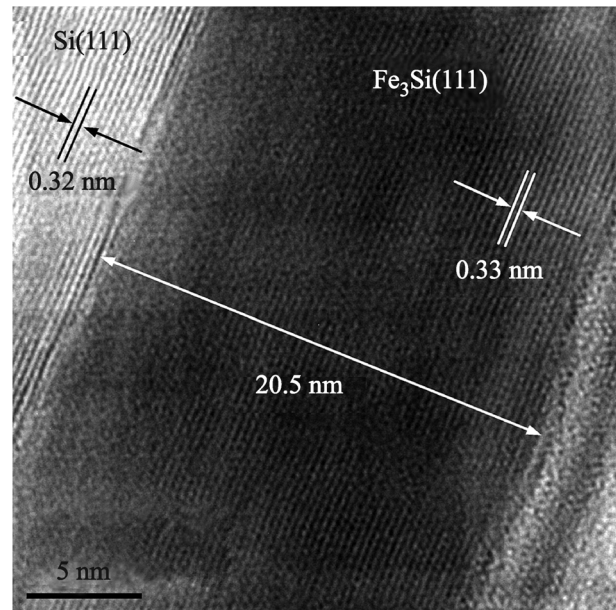


**Fig. 2.** Cross-sectional high resolution transmission electron microscopy image of the  $\text{Fe}_3\text{Si}/\text{Si}(111)$  structure.

scope. The analysis of the image confirms the epitaxial structure of the  $\text{Fe}_3\text{Si}$  film with the orientation  $\text{Si}[111] \parallel \text{Fe}_3\text{Si}[111]$ . Figure 2 shows the atomic  $\text{Si}(111)$  and  $\text{Fe}_3\text{Si}(111)$  planes. It was determined that the interplanar distance on the Si substrate was 0.32 nm, which is close to  $\text{Si}(111) = 0.314$  nm (PDF 4+ card #00-005-0565). The interplanar distance of the Si-Fe system was 0.33 nm, which is close to  $\text{Fe}_3\text{Si}(111) = 0.327$  nm (PDF 4+ card #00-015-3939) [9].

These results are confirmed by the data of the X-ray structural analysis. It was determined from them that the studied structure has a cubic symmetry  $Fm\bar{3}m$  with the unit cell parameter 0.564(3) nm close to the value for the bulk  $\text{Fe}_3\text{Si}$  crystal of 0.567 nm (PDF 4+ card #00-015-3939) [9].

The analysis of the X-ray structural data (see Fig. 3) indicates the presence of reflections from the substrate and one reflection with the coordinate  $2\theta = 27.3^\circ$  from the prepared film, which corresponds to the (111) plane of the  $\text{Fe}_3\text{Si}$  phase. The absence of other reflections of the  $\text{Fe}_3\text{Si}$  phase indicates that the texture of this film on the (111) plane is 100%. The origin of a step in the X-ray patterns in the region  $2\theta = 27.5^\circ$  is the usage of a Ni filter for the attenuation of the  $K_\beta$  radiation. The analysis of the half-width of the reflection showed that the minimum size of the crystalline  $\text{Fe}_3\text{Si}$  layer is 20 nm. This value is comparable with the film thickness.

**4.** The study of the magnetic properties of the  $\text{Fe}_3\text{Si}$  film using the method of ferromagnetic resonance showed the presence of both uniaxial ( $H_0$ ) and slight

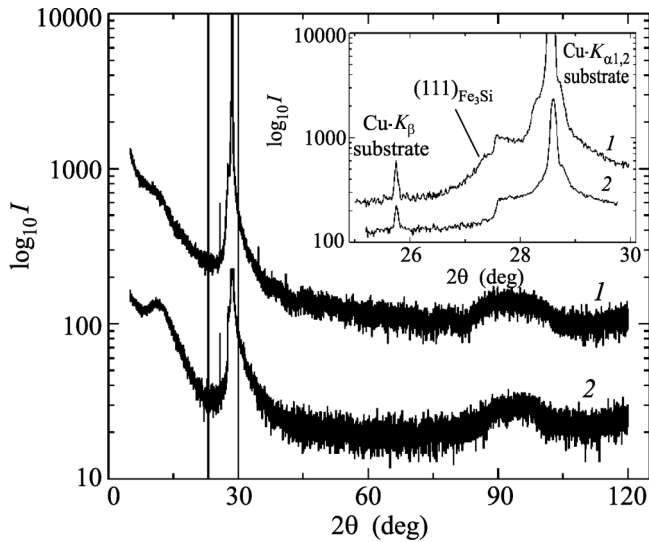


Fig. 3. X-ray patterns from  $\text{Fe}_3\text{Si}/\text{Si}(111)$  (1) and  $\text{Si}(111)$  (2).

unidirectional ( $H_{ua}$ ) anisotropy. Figure 4 shows the angular dependence of the resonance field  $H_R(\varphi)$  oriented in the film plane measured with a step of  $2^\circ$  on the scanning spectrometer of ferromagnetic resonance [14] at a pump frequency of 2.274 GHz.

To determine the main magnetic characteristics of the studied film from the angular dependences of the ferromagnetic resonance field, we used the phenomenological model in which the free energy density has the form [14]

$$F = F_Z + F_m + F_a + F_{ua},$$

where  $F_Z = -(\mathbf{M}\mathbf{H})$  is the Zeeman energy density,

$F_m = (\mathbf{M}\mathbf{N}\mathbf{M})/2$  is the magnetostatic energy density,

$F_a = -\frac{(\mathbf{M}\mathbf{H}_a)^2}{2M_s^2}$  is the density of the magnetic uniaxial

anisotropy energy,  $F_{ua} = -(\mathbf{M}\mathbf{H}_{ua})$  is the density of unidirectional anisotropy energy,  $\mathbf{H}$  is the static magnetic field strength,  $\mathbf{M}$  is the magnetization vector,  $\mathbf{N}$  is the tensor of the demagnetizing coefficients, and  $M_s$  is the saturation magnetization.

It is easy to obtain for such a model the theoretical dependence of the ferromagnetic resonance field on the angle of the direction of the magnetic sweep field  $\varphi$  from the solution of the Landau–Lifshitz equation. As a result of the iteration process, the saturation magnetization ( $M_s = 875$  G), the anisotropy field ( $H_a = 26$  Oe), and the field of the unidirectional anisotropy ( $H_{ua} = 0.9$  Oe) can be determined by fitting the magnetic film parameters so that the theoretical dependence  $H_R(\varphi)$  with the given accuracy coincides with that measured experimentally [14]. It is important to emphasize that the saturation magnetization in our

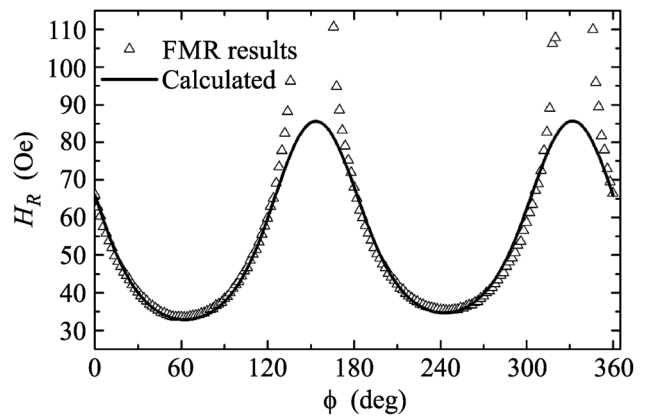


Fig. 4. Angular dependence of the resonance field  $H_R(\varphi)$  for the  $\text{Fe}_3\text{Si}/\text{Si}(111)$  structure.

case is higher than that for  $\text{Fe}_3\text{Si}$  grown on  $\text{Si}(111)$  ( $\sim 650$  G) in [8] and for  $\text{Fe}_3\text{Si}$  grown on  $\text{GaAs}(001)$  ( $\sim 790$  G) in [15] but is lower than the saturation magnetization for bulk  $\text{Fe}_3\text{Si}$  ( $\sim 1270$  G) [16]. In addition, the width of the ferromagnetic resonance line ( $\Delta H = 11.57$  Oe) and the coercive force ( $H_c = 12.3$  Oe) were measured. These magnetic characteristics are comparable with the magnetic characteristics of the film materials which are used in sensors of weak magnetic fields [17] and can be used as an active magnetic material in different electrically controlled devices of the microwave range (e.g., in filters, amplitude and phase modulators, and power limiters [18, 19]). During the synthesis of materials for such devices, high magnetic permeability and low losses of the microwave power are required. Therefore, the main aim is to increase the saturation magnetization  $M_s$  and to decrease the width of the ferromagnetic resonance line  $\Delta H$ .

5. To summarize, we have studied the structure prepared during the simultaneous evaporation from two iron and silicon sources on an atomically pure  $\text{Si}(111)7 \times 7$  surface at the substrate temperature of  $150^\circ\text{C}$ . This structure has been identified as single-crystal  $\text{Fe}_3\text{Si}$  silicide. It has been established that the prepared film has uniaxial magnetic anisotropy ( $H_a = 26$  Oe) and a relatively narrow uniform ferromagnetic resonance line ( $\Delta H = 11.57$  Oe) measured at a pump frequency of 2.274 GHz.

This work was supported by the Russian Foundation for Basic Research (project no. 13-02-01265), the Council of the President of the Russian Federation for Support of Young Scientists and Leading Scientific Schools (project no. NSh-2886.2014.2), and the Ministry of Education and Science of the Russian Federation (state contract no. 02G25.31.0043; state task of the Siberian Federal University for research in 2014).

## REFERENCES

1. S. A. Wolf, D. D. Awschalom, R. A. Buhrman, J. M. Daughton, S. von Molnar, M. L. Roukes, A. Y. Chtchelkanova, and D. M. Treger, *Science* **294**, 1488 (2001).
2. S. Datta and B. Das, *Appl. Phys. Lett.* **56**, 665 (1990).
3. R. R. Gareev, D. E. Bürgler, M. Buchmeier, R. Schreiber, and P. Grünberg, *J. Magn. Magn. Mater.* **240**, 235 (2002).
4. N. V. Volkov, A. S. Tarasov, E. V. Eremin, S. N. Varnakov, S. G. Ovchinnikov, and S. M. Zharkov, *J. Appl. Phys.* **109**, 123924 (2011).
5. B. T. Jonker, G. Kioseoglou, A. T. Hanbicki, C. H. Li, and P. E. Thompson, *Nature Phys.* **3**, 542 (2007).
6. S. R. Naik, S. Rai, M. K. Tiwari, and G. S. Lodha, *J. Phys. D: Appl. Phys.* **41**, 115307 (2008).
7. S. N. Varnakov, A. S. Parshin, S. G. Ovchinnikov, D. Rafaja, L. Kalvoda, A. D. Balaev, and S. V. Komogortsev, *Tech. Phys. Lett.* **31**, 947 (2005).
8. K. Hamaya, K. Ueda, Y. Kishi, Y. Ando, T. Sadoh, and M. Miyao, *Appl. Phys. Lett.* **93**, 132117 (2008).
9. Powder Diffraction File (PDF 4+, 2012), Inorganic Phases (International Center for Diffraction Data, Swarthmore, PA, USA, 2012).
10. S. N. Varnakov, A. A. Lapeshev, S. G. Ovchinnikov, A. S. Parshin, M. M. Korshunov, and P. Nevoral, *Instrum. Exp. Tech.* **47**, 839 (2004).
11. A. Ishizaka and Y. Shiraki, *J. Electrochem. Soc.* **133**, 666 (1986).
12. I. A. Tarasov, N. N. Kosyrev, S. N. Varnakov, S. G. Ovchinnikov, S. M. Zharkov, V. A. Shvets, and O. E. Tereshchenko, *Tech. Phys.* **57**, 1225 (2012).
13. S. M. Zharkov, E. T. Moiseenko, R. R. Altunin, N. S. Nikolaeva, V. S. Zhigalov, and V. G. Myagkov, *JETP Letters* **99**, 405 (2014).
14. B. A. Belyaev, A. V. Izotov, and A. A. Leksikov, *IEEE Sens. J.* **5**, 260 (2005).
15. K. Lenz, E. Kosubek, K. Baberschke, H. Wende, J. Herfort, H. P. Schönherr, and K. H. Ploog, *Phys. Rev. B* **72**, 144411 (2005).
16. H. P. J. Wijn, *Magnetic Properties of Metals: d-Elements, Alloys and Compounds* (Springer, Berlin, Heidelberg, New York, 1991).
17. A. N. Babitskii, B. A. Belyaev, and A. A. Leksikov, *Russ. Phys. J.* **55**, 861 (2013).
18. B. A. Belyaev, A. V. Izotov, S. Ya. Kiparisov, and G. V. Skomorokhov, *Phys. Solid State* **50**, 676 (2008).
19. V. G. Myagkov, V. S. Zhigalov, B. A. Belyaev, L. E. Bykova, L. A. Solovyov, and G. N. Bondarenko, *J. Magn. Magn. Mater.* **324**, 1571 (2012).

*Translated by L. Mosina*